

# Evidence for Thermally Activated Spontaneous Fluxoid Formation in Superconducting Thin-Film Rings

J. R. Kirtley and C. C. Tsuei

*IBM T.J. Watson Research Center, P.O. Box 218, Yorktown Heights, NY 10598*

F. Tafuri

*INFN-Coherentia Dip. di Ingegneria dell'Informazione,  
Seconda Università di Napoli, Aversa (CE), Italy*

(Dated: October 30, 2018)

We have observed spontaneous fluxoid generation in thin-film rings of the amorphous superconductor  $\text{Mo}_3\text{Si}$ , cooled through the normal-superconducting transition, as a function of quench rate and externally applied magnetic field, using a variable sample temperature scanning SQUID microscope. Our results can be explained using a model of freezout of thermally activated fluxoids, mediated by the transport of bulk vortices across the ring walls. This mechanism is complementary to a mechanism proposed by Kibble and Zurek, which only relies on causality to produce a freezout of order parameter fluctuations.

A number of years ago Zurek [1] proposed that condensed matter systems can be used as models for testing ideas, first introduced by Kibble[2, 3], concerning the quenching of topological defects in the early evolution of the universe. The principal picture developed by Kibble and Zurek was that, as a system approaches the critical temperature of a phase transition from above, the system slows down until at some temperature different regions cannot communicate with each other quickly enough to have correlated order parameters. As the transition proceeds further, fluctuations between different regions are “frozen in”, leading to relatively long-lived topological defects. Although this was only one of several mechanisms for freezout of topological defects considered by Kibble and Zurek, for brevity we will refer to this as the “Kibble-Zurek” mechanism in this paper. The advantage of using condensed matter systems to test these ideas is clear: while it is impossible to do experiments on a cosmological scale, there are a number of well understood phase transitions into macroscopic quantum states in condensed matter that are experimentally accessible.

The results of a number of experimental tests of these ideas have been mixed: Although vortex generation was at first observed in  $^4\text{He}$  upon rapid quenching into the superfluid state [4], a refinement of the original experiment by the same group [5] found a residual vortex density two orders of magnitude smaller than the Kibble-Zurek prediction. Experiments on vortex formation upon rapid quenching in  $^3\text{He}$  [6, 7] found good agreement with the Kibble-Zurek predictions. A search for spontaneous vortex generation in a bulk superconductor upon rapid quenching [8] was unsuccessful, although sensitivity of  $10^{-3}$  of the Kibble-Zurek prediction was reported. However, tests on superconducting loops interrupted by Josephson weak links have found good agreement with the Kibble-Zurek predictions, both for high- $T_c$  [9] and low- $T_c$  [10, 11, 12] superconductors.

In addition to the standard Kibble-Zurek mechanism,

which only relies on the satisfaction of the principle of causality to “freeze in” topological defects, it is also possible for thermally activated defects to appear and be trapped in the system during cooldown [1]. Detailed calculations of trapping of thermally activated fluctuations have been made in the hot Abelian Higgs model[13], and for the case of superconducting rings[14]. In this paper we report on measurements of spontaneous fluxoid formation in arrays of thin film superconducting rings with various ring dimensions and compositions. SQUID imaging of such arrays allowed the performance of a number of cooling experiments simultaneously. The film thicknesses and compositions were chosen to obtain large magnetic penetration depths and inductances, which produce favorable conditions for thermally activated behavior. The experiments provide evidence for the thermally activated appearance of topological defects (in this case vortices and antivortices) in systems undergoing a sufficiently rapid phase transition into an ordered state. We argue that such processes should be considered as a complementary mechanism in tests of the Kibble-Zurek predictions.

Although we obtained qualitatively similar results on rings fabricated from the low- $T_c$  superconductor Nb, and the cuprate superconductor  $\text{YBa}_2\text{Cu}_3\text{O}_{7-\delta}$ , we will report in this paper on thin-film ( $d=50\text{nm}$ ) rings of the amorphous superconductor  $\text{Mo}_3\text{Si}$ [15], which showed the largest spontaneous fluxoid generation, and on which the most detailed measurements were taken. The films were fabricated by rf-sputtering on sapphire substrates and photolithographically defined using ion-beam etching. Results will be presented here on two sets of rings. One set consisted of 25 circular rings, with inside diameter  $2a=40\ \mu\text{m}$  and outside diameter  $2b=80\ \mu\text{m}$ , spaced by  $160\ \mu\text{m}$  in a  $5\times 5$  square array. The second set had 144 rings with  $2a=20\ \mu\text{m}$  and  $2b=30\ \mu\text{m}$ , spaced by  $60\ \mu\text{m}$  in a  $12\times 12$  square array. The films had a resistive superconducting critical temperature  $T_c=7.81\ \text{K}$ , with a transition width (10%-90%)  $\Delta T_c=0.03\ \text{K}$  wide. Magnetic

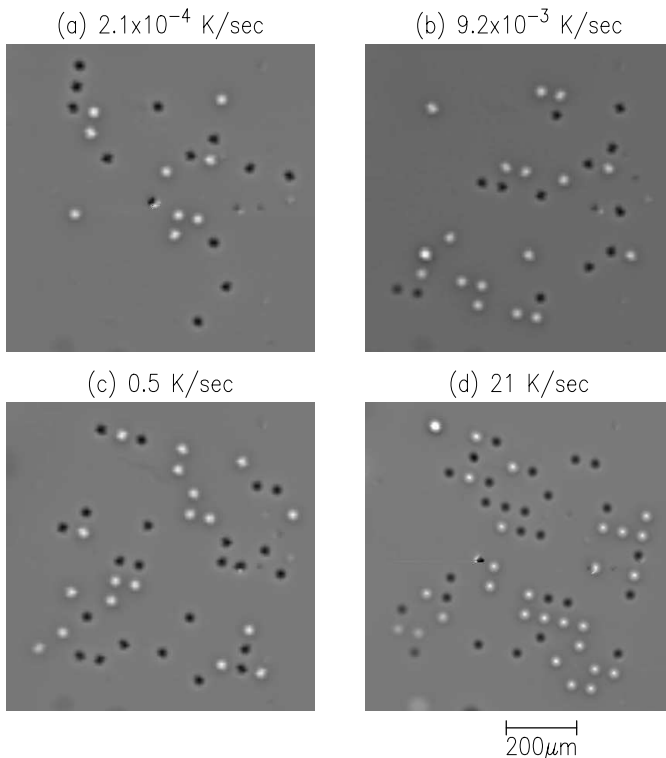


FIG. 1: Scanning SQUID microscope images of a  $12 \times 12$  array of  $20 \mu\text{m}$  inside diameter,  $30 \mu\text{m}$  outside diameter thin film rings of  $\text{Mo}_3\text{Si}$ , cooled in zero field through the superconducting  $T_c$  at various rates, and imaged with an  $8 \mu\text{m}$  square pickup loop. The full scale variation of the grey scale images corresponded to  $0.25\Phi_0$  (a),  $0.3\Phi_0$  (b),  $0.25\Phi_0$  (c), and  $0.37\Phi_0$  (d) change in flux through the pickup loop. The principal axes of the square array are rotated by  $12^\circ$  clockwise with respect to the image frame.

imaging measurements were made with a variable sample temperature, scanning SQUID microscope[16], with a square pickup loop  $8 \mu\text{m}$  on a side. The sample was mounted with a thin layer of GE varnish on a sapphire substrate to which a silicon diode thermometer and non-inductive resistive heater were attached. Both sample and SQUID were inside an evacuated can surrounded by liquid  $^4\text{He}$ . The thermal time constant of the sample mount was varied by changing the amount of  $^3\text{He}$  exchange gas between it and the  $^4\text{He}$  bath. Fits to SQUID images of the rings with fluxoid number  $N=1$  at zero field gave a Pearl length [17]  $\Lambda=2\lambda_L^2/d$  ( $\lambda_L$  the London penetration depth)  $=7 \mu\text{m}$  at  $4.4 \text{ K}$ .

Our experiments consisted of cooling the sample in a given field at a controlled rate, and then imaging the rings with the SQUID microscope to determine the final fluxoid state. The spacing between rings was large enough that ring-ring interactions were not important in the cooldown dynamics.

Figure 1 shows SQUID microscope images of the  $20$

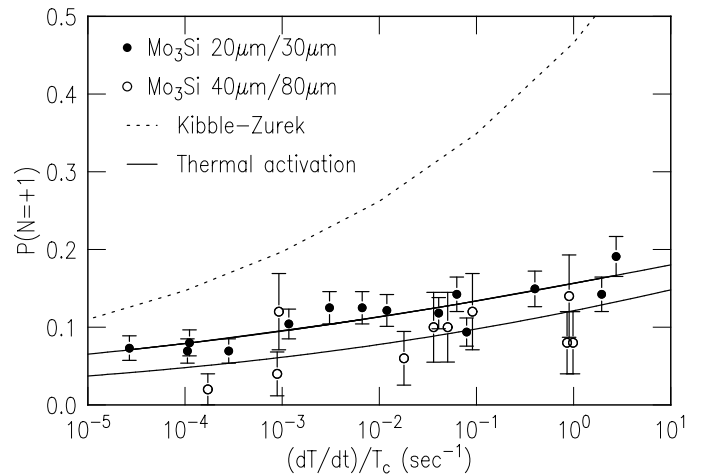


FIG. 2: Probability of  $20 \mu\text{m}$  inside diameter,  $30 \mu\text{m}$  outside diameter  $\text{Mo}_3\text{Si}$  rings (closed symbols) and  $40 \mu\text{m}/80 \mu\text{m}$  rings (open symbols) having a final fluxoid number of  $+1$ , as a function of the cooling rate, after cooling in zero externally applied magnetic flux. The dashed line is the prediction of the Kibble-Zurek quenched disorder model, and the solid lines are fits to the frozen thermally activated bulk vortex model discussed in the text.

$\mu\text{m}/30 \mu\text{m}$  ring array, cooled through  $T_c$  at zero field with varying cooling rates. In this image the rings with final fluxoid number  $N=0$  are not visible; rings with positive fluxoid number (counter-clockwise circulating supercurrents) are white; and those with negative fluxoid number (clockwise supercurrents) are black. Most of the rings with non-zero fluxoid number have  $N=+1$  or  $-1$ , but a few rings also have  $N=+2$  or  $-2$ . For example, the upper left most ring in Fig. 1 (d) has  $N=2$ .

Figure 2 displays the results, plotted as the probability for a ring to be in the  $N=+1$  fluxoid state, for a number of cooling rates, for both ring sizes. The error bars are assigned by setting the standard deviation of the number of  $N=+1$  rings to be the square root of the number of  $N=+1$  rings observed in each experiment. This plot shows that  $P(N=+1)$  varies roughly linearly with the logarithm of the cooling rate.

The Kibble-Zurek prediction for the expected fluxoid number for a quenched superconducting ring due to freeze-out of order parameter fluctuations is [1]

$$N = \frac{1}{2\pi} \sqrt{C/\xi_0} (\tau/\tau_Q)^{\frac{1}{2}}, \quad (1)$$

where  $C$  is the circumference of the ring,  $\xi_0$  is the zero temperature coherence length,  $\tau = \pi\hbar/16k_B T_c$  is the Ginzburg-Landau relaxation time, and  $\tau_Q^{-1} = |dT/dt|/T_c$  is the normalized cooling rate. The dashed curve in Fig. 2 is this prediction for the  $20 \mu\text{m}/30 \mu\text{m}$  rings, using  $\xi_0=4.9\text{nm}$ [18], and taking  $C$  to be the inside circumference of the rings. The corresponding prediction

for the 40  $\mu\text{m}/80 \mu\text{m}$  rings would be scaled vertically by a factor of  $\sqrt{2}$ . The Kibble-Zurek mechanism predicts more spontaneous fluxoid generation than is observed, as well as a strong increase with ring size which is not observed. Moreover, the Kibble-Zurek prediction, although it has a weak  $(T_c^{-1} |dT/dt|)^{1/8}$  dependence, nevertheless varies more rapidly with cooling rate than experiment. We should note that the Kibble-Zurek predictions for a superconducting ring were for ring walls much thinner than the ring diameter[1]. However, we do not believe that our finite ring wall widths would effect the Kibble-Zurek predictions qualitatively.

We suggest that our observed logarithmic dependence of non-zero fluxoid probability on cooling rate is due to spontaneous changes in the ring fluxoid number by thermal activation in, and transport across, the ring wall of bulk vortices. Such a model has been used to qualitatively explain measurements on telegraph noise and fluxoid transition rates in superconducting thin-film rings of underdoped cuprate  $\text{Bi}_2\text{Sr}_2\text{CaCu}_2\text{O}_{8-\delta}$ [19, 20], which have penetration depths and coherence lengths comparable to the present samples. Physically our picture is that, as the rings cool through  $T_c$  thermally activated fluctuations rapidly change the fluxoid number. The thermal activation barrier to this process becomes large as the temperature is reduced further, eventually turning this process off, leaving the rings with some probability of being in energetically excited states.

We calculate the probability  $P_N$  of a ring being in the  $N$ th fluxoid number state as follows: Consider a set of ring fluxoid states  $N$ , with ring energies  $E_N$ , and with barrier energies  $E_B$  (in our model the energy required to nucleate a vortex in the ring wall) that must be overcome to make the transition between them. The transition rate  $\nu_{N \rightarrow N'}$  is given by

$$\nu_{N \rightarrow N'} = P_N \nu_0 e^{-(E_B - E_N)/k_B T}, \quad (2)$$

where  $\nu_0$  is an attempt frequency, and we neglect the dependence of the transition rate on the final state energy. At high temperatures, in equilibrium,  $\nu_{N \rightarrow N'} = \nu_{N' \rightarrow N}$  for all  $N, N'$ . This implies that

$$P_N = e^{-E_N/k_B T} / \sum_{N'} e^{-E_{N'}/k_B T}. \quad (3)$$

The ring energies  $E_N = E_r(N - \phi_a)^2$ , with  $\phi_a = \Phi_a/\Phi_0$  the normalized externally applied flux, and  $\Phi_0 = hc/2e$  the superconducting flux quantum[21]. Eq. 3 implies that the probability of a ring having a non-zero fluxoid number depends on the ratio  $E_r/k_B T$ . As the ring cools down, the transition rates slow down when  $E_B(T) \simeq k_B T$ , fixing the ring fluxoid number. We can assign a ‘‘freezing’’ temperature  $T_F$  by insisting that the probability of there being a further fluxoid jump, obtained by integrating the transition rates over temperature from  $T=T_F$  to  $T=0$ , be less than 1. It can then be

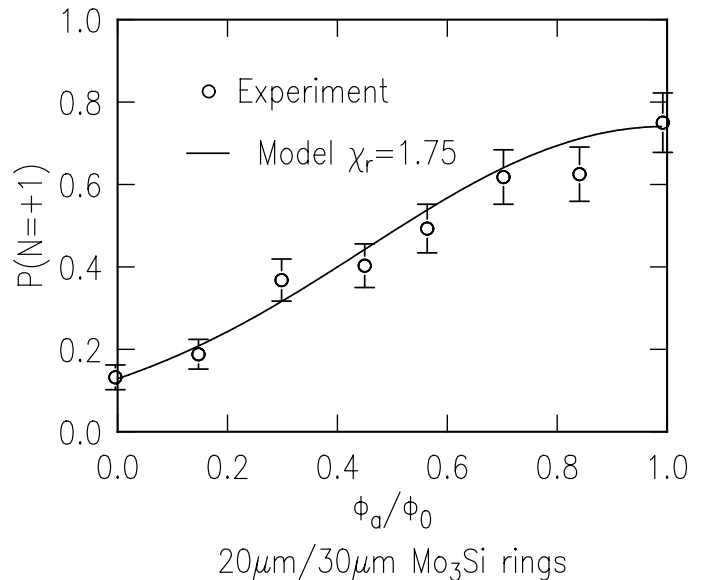


FIG. 3: Probability of 20  $\mu\text{m}$  inside diameter, 30  $\mu\text{m}$  outside diameter  $\text{Mo}_2\text{Si}$  rings having a final fluxoid number of +1, as a function of the externally applied magnetic flux. The open symbols are the data, the solid line is a fit to the thermally activated vortex model discussed in the text.

shown that

$$k_B T_F = -E_B(T_F) / \ln \left( \frac{\gamma |dT/dt|}{k_B \nu_0 T_F} \right), \quad (4)$$

where  $\gamma = dE_B(T)/dT |_{T=T_F}$ . We then rewrite Eq. 3 to obtain the probability  $P_{N,F}$  that a ring is frozen into a state with fluxoid number  $N$ :

$$P_{N,F} = e^{-\chi_r(N - \phi_a)^2} / \sum_{N'} e^{-\chi_r(N' - \phi_a)^2}, \quad (5)$$

with  $\chi_r \equiv E_r(T_F)/k_B T_F$ . For the parameters of our system,  $P_{N,F}$  varies nearly linearly with  $\chi_r$ , and therefore depends roughly logarithmically on cooling rate through Eq. 4.

The upper solid line in Fig. 2 is a fit of Eq. 5 to the 20  $\mu\text{m}/30 \mu\text{m}$  ring data, resulting in best fit values of  $E_r(T_F)/E_B(T_F) = 0.097 \pm 0.1$  and  $\gamma/k_B \nu_0 = 2.4 \times 10^{-7}$  sec., with upper and lower limits of  $17.5 \times 10^{-7}$  sec. and  $0.4 \times 10^{-7}$  sec. respectively on the latter value, using a doubling of  $\chi^2$  as a criterion. In the temperature range of interest,  $1-t=(T_c-T)/T_c \ll 1$ , the Pearl length  $\Lambda(T) \simeq \Lambda(0)/(1-t^4)$  is larger than typical ring dimensions. In this limit[20]

$$E_r(\Lambda > a, b) \simeq \Phi_0^2 / (8\pi^2 \Lambda). \quad (6)$$

The energy  $E_B$  required to nucleate a vortex in a thin film strip of width  $W$  is given by [22]

$$E_B = \frac{\Phi_0^2}{8\pi^2 \Lambda} \ln \left( \frac{2W}{\pi \xi} \right). \quad (7)$$

Combining Eq.'s 6 and 7 we estimate  $E_r/E_B \approx 1/\ln(2W/\pi\xi)$ . Using Eq. (7), Eq. (4),  $\Lambda(0)=7 \mu\text{m}$ ,  $\xi(T) = \xi(0)/\sqrt{1-t}$ , and  $W = b - a = 5 \mu\text{m}$ , leads to  $(T_c - T_F)/T_c = 2 \times 10^{-3}$ ,  $\gamma=2.7 \times 10^{-14}$  erg/K, leading to  $E_r/E_B=0.30$ , a factor of three larger than our fit value. Our fit value for  $\gamma/k_B\nu_0$  implies  $\nu_0=8.3 \times 10^8$  sec.<sup>-1</sup>, with upper and low limits of  $6.1 \times 10^9$  sec.<sup>-1</sup> and  $1.1 \times 10^8$  sec.<sup>-1</sup> respectively, in reasonable agreement with attempt frequencies obtained from fluxoid dynamics of  $\text{Bi}_2\text{Sr}_2\text{CaCu}_2\text{O}_{8-\delta}$  rings with similar penetration depths [19, 20]. The lower solid line in Fig. 2 is a fit to the 40  $\mu\text{m}/80 \mu\text{m}$  ring data, using the value for  $\gamma/k_B\nu_0$  obtained from the 20  $\mu\text{m}/30 \mu\text{m}$  rings, and allowing  $E_r(T_F)/E_B(T_F)$  to vary. The best fit value in this case is  $E_r(T_F)/E_B(T_F)=0.12$ , with upper and lower limits of 0.15 and 0.105, to be compared with a calculated estimate for these rings of  $E_r/E_B=0.2$ . Note, however, that the predicted dependence on wall width does not match the experimental results: doubling the size of the ring wall should decrease the value for  $E_r/E_B$  by 30%, but our fit values increase by about that amount.

A further test of our model is provided by measurements of the final state fluxoid number probability as a function of applied field. Figure 3 shows the results of such experiments for the 20  $\mu\text{m}/30 \mu\text{m}$  rings, cooled at a cooling rate of 15 K/sec. At first these results are startling: the fluxoid number probabilities depend only weakly on applied field. This is in contrast to pioneering work by Davidović et al. [23, 24] on 1.6  $\mu\text{m}$  outside diameter thin film aluminum rings, which showed, e.g.  $P_{1,F}$  stepping up sharply from 0 to 1 at  $\phi_a=0.5$ . This difference can be explained qualitatively as follows: our rings, which have large values for  $a, b$ , and  $\Lambda$ , have small ring energy spacings (scaled by  $E_r$ ). Therefore  $k_B T_F$  is comparable to  $E_r(T_F)$  and it is probable that energetically unfavorable final fluxoid numbers will be populated. On the other hand, the rings of Davidović have much smaller values for  $a, b$ , and  $\Lambda$ , and the ring energy spacings will be correspondingly larger. The solid line in Fig. 3 is a fit to the data using Eq. 5, with  $\chi_r$  as a fitting parameter. The best fit is obtained for  $\chi_r = 1.75$ , compared to a value of 4.3 calculated from Eq. 4.

In conclusion, we have found that our results for the spontaneous generation of energetically unfavorable final fluxoid numbers in cooled thin-film rings of the amorphous superconductor  $\text{Mo}_3\text{Si}$  can be explained using a model of thermally activated bulk vortices. This mechanism occurs over a much different time and temperature scale than the conventional Kibble-Zurek mechanism, which predicts that freezout of order parameter fluctuations occurs at  $\hat{\epsilon} \equiv |(T - T_c)/T_c| = \sqrt{\tau_0/\tau_Q} \approx 1 \times 10^{-7}$ . For our rings the thermally activated processes persist to  $\hat{\epsilon} \approx 1 \times 10^{-3}$ . In this case any fluxoids generated by the conventional Kibble-Zurek mechanism would be “washed out” by the thermally activated vortex mechanism. Our

rings are exceptionally susceptible to thermally activated vortex processes: they have very large magnetic penetration depths and inductances, which make nucleation of vortices not too energetically costly at temperatures relatively far from  $T_c$ . Nevertheless, the possibility of thermally activated processes should be considered, keeping in mind that not only short coherence lengths, but also short penetration depths, are desirable when using superconductors for tests of the Kibble-Zurek mechanism for topological defect formation in quenched macroscopic quantum systems.

We would like to thank V.G. Kogan, and K.A. Moler for useful discussions during the course of this work. F.T. acknowledges the support of the ESF Project “VOR-TEX”.

- 
- [1] W.H. Zurek, Physics Reports 276, 177 (1996).
  - [2] T.W.B. Kibble, J. Phys. A9, 1387 (1976).
  - [3] T.W.B. Kibble, Phys. Rep. 67, 183 (1980).
  - [4] P.C. Hendry, N.S. Lawson, R.A.M. Lee, P.V.E. McClintock, and C.D.H. Williams, Nature 368, 315 (1994).
  - [5] M.E. Dodd, P.C. Hendry, N.S. Lawson, P.V.E. McClintock, and C.D.H. Williams, Phys. Rev. Lett. 81, 3703 (1998).
  - [6] C. Bäuerle, Yu. M. Bunkov, S.N. Fisher, H. Godfrin, and G.R. Pickett, Nature 382, 332 (1996).
  - [7] V.M.H. Ruutu, V.B. Eltsov, A.J. Gill, T.W.B. Kibble, M. Krusius, Yu. G. Makhlin, B. Plaçais, G.E. Volovik, and Wen Xu, Nature 382, 334 (1996).
  - [8] R. Carmi and E. Polturak, Phys. Rev. B 60, 7595 (1999).
  - [9] R. Carmi, E. Polturak, and G. Koren, Phys. Rev. Lett. 84, 4966 (2000).
  - [10] E. Kavoussanaki, R. Monaco, and R.J. Rivers, Phys. Rev. Lett. 85, 3452 (2000).
  - [11] R. Monaco, J. Mygind, and R.J. Rivers, Phys. Rev. Lett. 89, 080603 (2002).
  - [12] R. Monaco, J. Mygind, and R.J. Rivers, preprint.
  - [13] M. Hindmarsh and A. Rajantie, hep-ph/0103311 (2001).
  - [14] M. Ghinovker, B. Ya. Shapiro, and I. Shapiro, Europhys. Lett. 53, 240 (2001).
  - [15] C.C. Tsuei, “Amorphous Superconductors”, in Encyclopedia of Magnetic and Superconducting Materials, edited by J. Evetts (Pergamon Press, 1992) p. 32.
  - [16] J.R. Kirtley *et al.*, Appl. Phys. Lett. 74, 4011 (1999).
  - [17] J. Pearl, J. Appl. Phys. **37**, 4139 (1966).
  - [18] A.V. Samoilov, N.-C. Yeh, and C.C. Tsuei, Phys. Rev. B 57, 1206 (1998).
  - [19] J.R. Kirtley, C.C. Tsuei, H. Raffy, Z.Z. Li, V.G. Kogan, J.R. Clem, and K.A. Moler, cond-mat/0103474.
  - [20] J.R. Kirtley, C.C. Tsuei, V.G. Kogan, J.R. Clem, H. Raffy, and Z.Z. Li, pre-print.
  - [21] A. Barone and G. Paterno, *Physics and Applications of the Josephson Effect*, Wiley, New York, 1982, p. 355.
  - [22] V.G. Kogan, Phys. Rev. B 49, 15874 (1994).
  - [23] D. Davidović *et al.*, Phys. Rev. Lett. 76, 815 (1996).
  - [24] D. Davidović *et al.*, Phys. Rev. B 55, 6518 (1997).